science, engineering and health studies

Research Article

Science, Engineering and Health Studies
https://li01.tci-thaijo.org/index.php/sehs
ISSN (Online): 2630-0087

Design and fabrication of low-cost capacitive sensors for salinity level detection in water

Chayanika Sharma[*], *Riki Baruah, Anandita Dey, Debashis Saikia, and Utpal Sarma*

Department of Instrumentation & USIC, Gauhati University, Assam 781014, India

***Corresponding author**:
Chayanika Sharma
chayanika114@gmail.com

***Received**: 12 April 2023*
***Revised**: 26 September 2023*
***Accepted**: 14 October 2023*
***Published**: 29 December 2023*

***Citation**:
Sharma, C., Baruah, R., Dey, A., Saikia, D., and Sarma, U. (2023). Design and fabrication of low-cost capacitive sensors for salinity level detection in water. Science, Engineering and Health Studies, 17, 23020010.*

ABSTRACT

The salinity of water has a negative impact on both climate change as well as human health. Therefore, the in situ monitoring of water salinity is important. Numerous approaches, including electromagnetic inductive sensing, remote sensing, methods based on optical fiber sensors, conductive sensing (capacitive or resistive), can be used to measure the salinity of the water. This work focuses mainly on the design and fabrication of low-cost co-planar interdigitated (IDT) sensors with sensitive fringing field measurement capabilities. IDT sensors with configurations 1-1-1, 1-3-1, 1-7-1, and 1-15-1 were designed and fabricated in this work. The capacitance values for all four configurations decrease proportionally with water salinity, demonstrating a negative linear response in sensors that utilize water salinity levels as the dielectric media.

Keywords: IDT sensor; water salinity; fringing field

1. INTRODUCTION

Assessment of water salinity in the sources of irrigation water (Baath et al., 2017), as well as drinking water (Akter, 2019) has become an important task as it imposes many direct and indirect implications on climate change (Corwin, 2021). The causes of water salinity can be natural or human-induced. Salinity in irrigation water causes salts to accumulate in the soil over a long period. These soils contain more electrolytes than any other type of soil, both in their liquid and solid states. Due to this, various problems like inhibition of plant growth, change in soil properties, and contamination of ground water occur (Mohanavelu et al., 2021). Irrigation water containing salt reduces overall crop yield and growth in salt–intolerant crops (Sharma et al., 2023). Similarly, it causes the death of aquatic organisms that rely on specific salinity levels to survive in their natural habitat, and it can be the cause of native vegetation death or poor health. These are factors causing a decline in biodiversity (Briggs and Taws, 2003; Rahman et al., 2011). However, the impact of salinity in drinking water has become another growing medical concern in many coastal areas. Scientists have investigated several correlations among the post-natal impacts of pre-natal salinity exposure through drinking water in terms of preeclampsia, postpartum depression, and infant mortality and morbidity (Dasgupta et al., 2016; Rahimi et al., 2021).

Several methods can be employed to determine the presence of salt in the water such as remote sensing methods (Metternicht and Zinck, 2003) (including multi-temporal optical and microwave signals), optical fiber sensor-based methods (Qian et al., 2018), conductive sensing methods (capacitive or resistive)

(Peddinti et al., 2020), and electromagnetic inductive sensing methods (Wu et al., 2015). Among these techniques, the capacitive type sensing method has been adopted by many researchers due to its low cost and easy fabrication procedures. When salt is present in water, the dielectric value of the water changes based on the amount of available salt. Consequently, when a capacitive-type sensor is placed in a saltwater medium, the capacitance value deviates from the normal baseline value obtained using distilled water (Gadani et al., 2012).

Sensors based on capacitive sensing operate on the principle of the dielectric which is mostly fabricated with parallel, coaxial, cylindrical, or co-planar arrangements. The design of a parallel plate capacitor is the simplest among them all. However, in this kind of capacitor, the electric field gets trapped in the area between the parallel plates and provides a result with little interference from the external media or objects. The cylindrical configuration involves difficult steps while depositing a uniform layer of electrodes. To overcome these problems, the co-planar type interdigitated (IDT) conductivity sensor is used for obtaining the information on the test media (Bhat, 2005).

The planar IDT sensors can be fabricated by placing n number of electrodes, i.e., parallel plates with parallel connections. The front surfaces of the electrodes are exposed to the substances being tested. This simplest IDT architecture offers the ability to measure fringing fields with extreme sensitivity (Islam et al., 2021). The overall capacitance of the sensors is affected by the geometry of the electrodes, thickness, spacing between them, the total number of parallel electrodes, and the substance being tested (Goswami et al., 2018; Mizuguchi et al., 2015).

In this study, IDT sensors with sensitive fringing field measurement abilities have been designed, simulated, and fabricated. A detailed investigation of different configurations of the IDT sensors has been carried out using the finite element method (FEM). The designed sensors were later fabricated and used to measure different levels of salinity present in the water. A proper signal conditioning circuit was designed to record the responses of the fabricated sensors in usable electrical form.

2. MATERIALS AND METHODS

2.1 Design procedures

2.1.1 IDT sensor design and simulation

The 17 fingered IDT capacitive sensors with equally spaced working and sensing electrodes were designed using the FEM in COMSOL Multiphysics software and simulated for different configurations. The sensor patterns 1-1-1, 1-3-1, 1-7-1, and 1-15-1, designed for simulation, were named as $C_1, C_3, C_7,$ and C_{15}. The fringing field effects for the capacitive sensors were simulated with air as the surrounding medium of the fingers and are shown in Figure 1. The working electrode was connected to a higher value of electric potential with respect to the sensing electrode. Because of this, the fringing field was generated from the working electrode that goes to the sensing electrode. Later in the simulation model, the parameters of the sensors, like the gap between the two electrodes (2g) and the width of the electrodes (w) for each configuration, were varied to monitor the change in capacitance with air as the dielectric medium prior to fabrication of the sensors. In Figure 2, the equivalent capacitance value generated for configuration C_1 is shown. In the same way, the capacitance value for each configuration can be calculated. From Figure 3, it is seen that as the ratio between w and 2g (w/2g) increases, the capacitance value also increases.

The equivalent capacitance values obtained for each configuration are calculated using Equations (1)–(4).

$$C_1 = 16(C_{1,1}) \quad (1)$$

$$C_3 = 8(C_{1,1} + C_{1,2} + C_{1,3}) \quad (2)$$

$$C_7 = 4(C_{1,1} + C_{1,2} + C_{1,3} + \cdots + C_{1,7}) \quad (3)$$

$$C_{15} = 2(C_{1,1} + C_{1,2} + C_{1,3} + \cdots + C_{1,15}) \quad (4)$$

In general, Equation (5) can be used for calculating the equivalent capacitance.

$$C_n = 2(x+1)(C_{1,1} + C_{1,2} + C_{1,3} + \cdots + C_{1,n}) \quad (5)$$

where x is the total number of interior working electrodes.

2.1.2 Fabrication of the IDT sensors

CAD software was used to design IDT sensors $C_1, C_3, C_7,$ and C_{15}, which contained 1, 3, 7, and 15 sensing electrodes, respectively, sandwiched between two working electrodes. The sensors were fabricated (with w/2g=2) using printed circuit board technology (PCB) on a single-layer FR4 board. The dimensions of the IDT sensor designs are listed in Table 1. The IDT capacitive sensors fabricated in this research work are shown in Figure 4.

2.1.3 Signal conditioning circuit

There are several methods to calculate capacitance, including the bridge-based method, charge-discharge method, direct micro-controller interfacing method, capacitance-to-digital conversion method, and the charge-to-voltage conversion method (Goswami and Sarma, 2015). In this work, the authors used a simple charge-to-voltage converter circuit (shown in Figure 5) to measure the equivalent capacitance generated by the fabricated IDT sensors. A charge-to-voltage converter circuit uses a charge transducer like a capacitive transducer to provide the change in charge ($\triangle Q$) as a function of a change in capacitance ($\triangle C$) (Master, 2010). The fabricated capacitive sensors were excited with AC signals (V_C) at different frequencies. Finally, the generated output voltages for each configuration of sensors were measured with the help of an oscilloscope.

The output voltage (V_{out}) of the circuit can be represented as per Equation (6).

$$V_{out} = \frac{-\Delta Q}{C_2} = \frac{-\Delta C.V_C}{C_2} \quad (6)$$

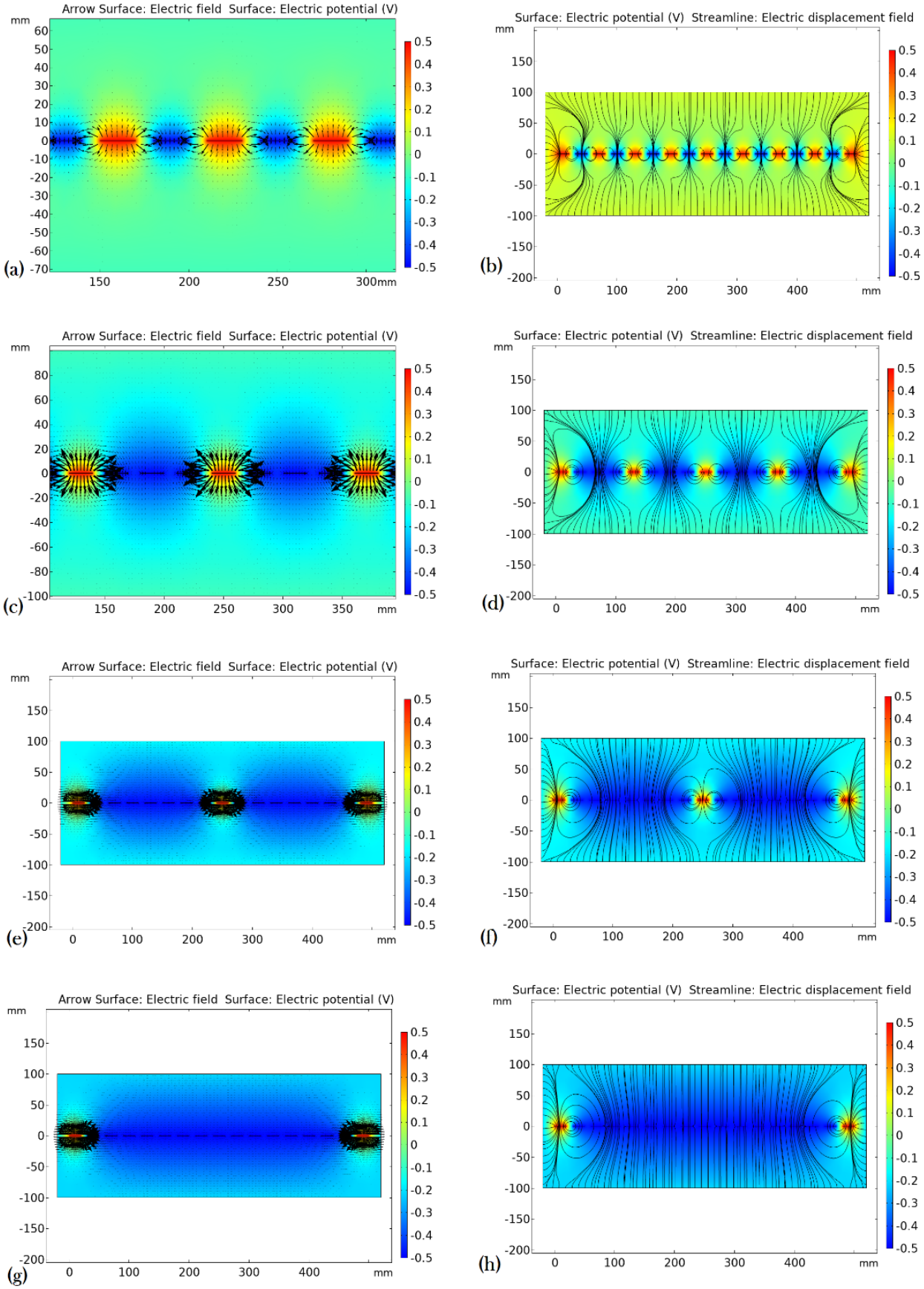

Figure 1. Simulation for fringing field effects of the configuration (a)–(b) C_1, (c) – (d) C_3, (e) – (f) C_7, and (g)– (h) C_{15}

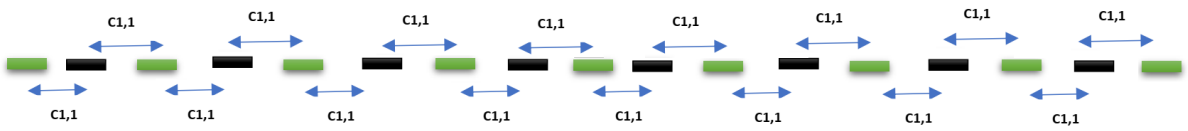

Figure 2. Equivalent capacitance for 1-1-1 pattern

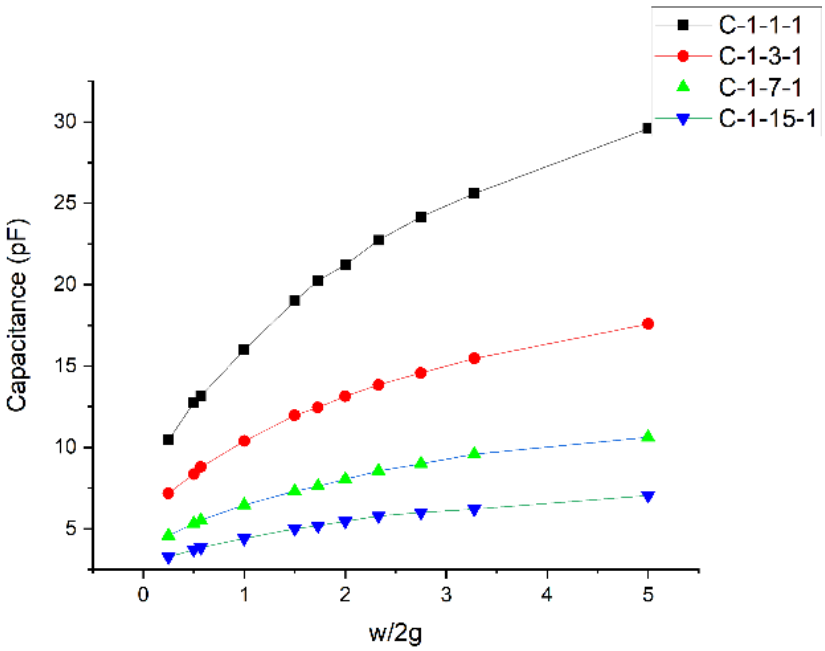

Figure 3. The equivalent capacitance values of the sensors calculated for different structures as a function of w/2g ratio in air

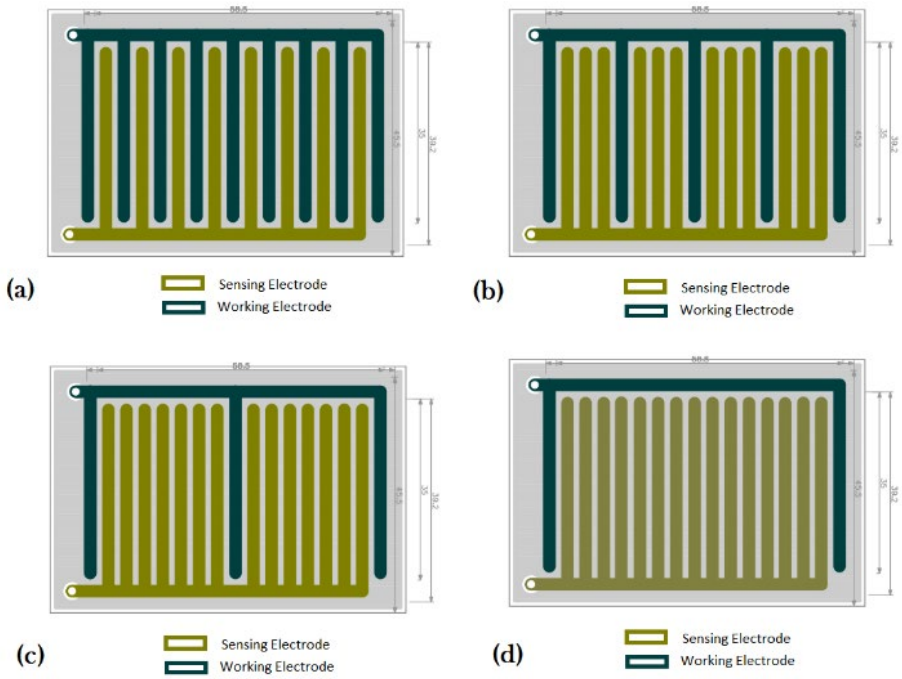

Figure 4. Patterns of the fabricated IDT sensors with 17 total fingers and w/2g=2 for (a) C_1, (b) C_3, (c) C_7, and (d) C_{15}

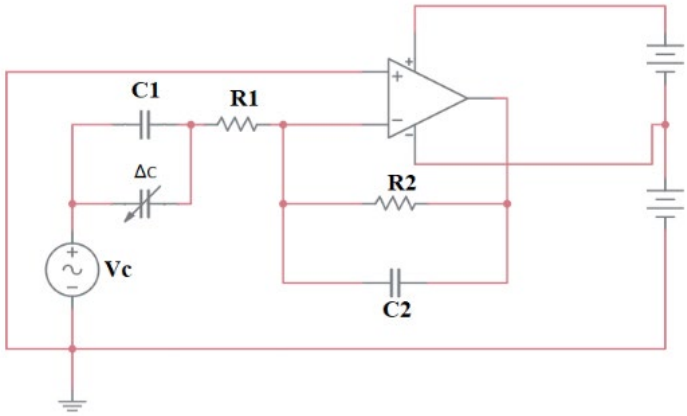

Figure 5. The analog front-end circuit used to convert the charge generated by the IDT sensors to voltage

Table 1. The dimensions of the fabricated sensors

Parameter	Dimension
Thickness of the FR4 board	1.5 mm
Thickness of the Cu layer	35.0 µm
Length of the electrodes	35.0 mm
Width of the electrodes(w)	2.0 mm
Gap between the two electrodes (2g)	1.0 mm

2.2 Experimental Details

To take the measurements, the sensors were placed inside a 250-mL beaker with different types of water serving as the dielectric medium, as shown in Figure 6. The water level height inside the beaker was kept at 150 mL during the measurements.

To create the salinity levels of 3 dS/m, 6 dS/m, 9 dS/m, 12 dS/m, and 16 dS/m, 2.25 g, 4.50 g, 6.75 g, 9.00 g, and 12.00 g of NaCl were dissolved, respectively, in 1 L of distilled water (Alam et al., 2020).

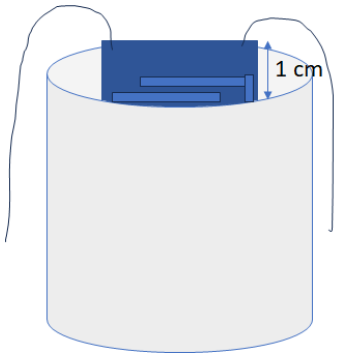

Figure 6. Placement of the sensor

3. RESULTS AND DISCUSSION

The responses of the constructed IDT sensors were observed using the aforementioned charge-to-voltage converter circuit. The capacitance of the sensors was altered using various dielectric mediums, including air, tap water, drinking water, distilled water, and water with different salinity levels. However, by exciting the IDT sensors with various frequencies, the resulting output voltages of the sensors were recorded.

The output voltage calculated for different configurations of the capacitive sensors using air as the dielectric medium is shown in Figure 7, which supports the simulation results, i.e., the output value observed for configuration 1-1-1 is the highest and the output value observed for configuration 1-15-1 is the lowest.

The fabricated sensor configurations have been tested using water with different salinity levels as dielectric medium to conduct further experimentation. Different salt-water concentrations were made using sodium chloride (NaCl) and distilled water.

The responses of the sensors at different salinity levels are provided in Figure 8. From the plot, it is seen that the sensors show a negative linear response with the applied salinity levels as a dielectric medium. A dielectric decrement is observed with the salt concentration of water. The addition of NaCl to water results in a drop in the dielectric constant, leading to a decrease in the capacitance of the designed sensor arrangements.

In Figure 9, the output voltages obtained for each sensor configuration excited at different frequencies are displayed. It can be inferred that out of the three types of water, tap water offers the largest value of output capacitance, while distilled water offers the lowest. Tap water and drinking water may contain various additional components, leading to different dielectric values when applied to the fabricated gas sensors. As a result, the output voltages obtained in each case varied.

Based on the experimental results, the equations for determining the change in capacitance of the fabricated sensor with respect to different concentrations of salinity levels at 20 kHz frequency were calculated, and are presented in Table 2. The graphs used for calculating these equations are shown in Figure 10.

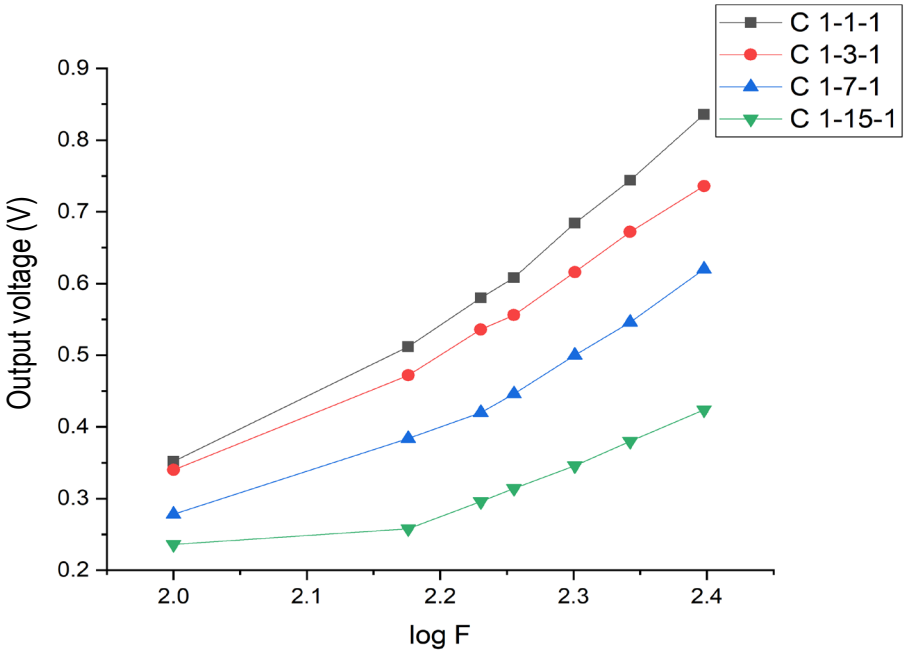

Figure 7. The output voltage value calculated for different structures excited at different frequencies in air

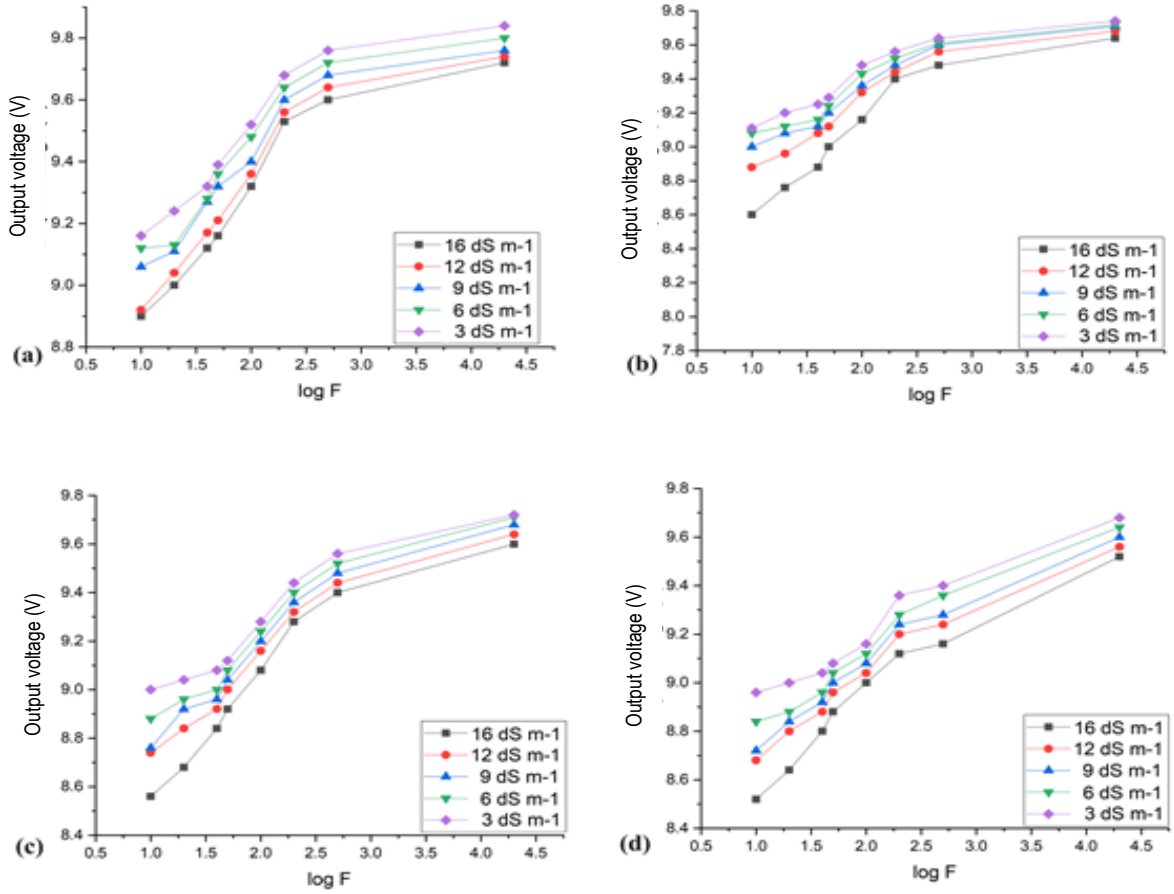

Figure 8. Frequency vs. output voltage plot using water with five different level of salinity as dielectric for (a) C_1, (b) C_3, (c) C_7, and (d) C_{15}

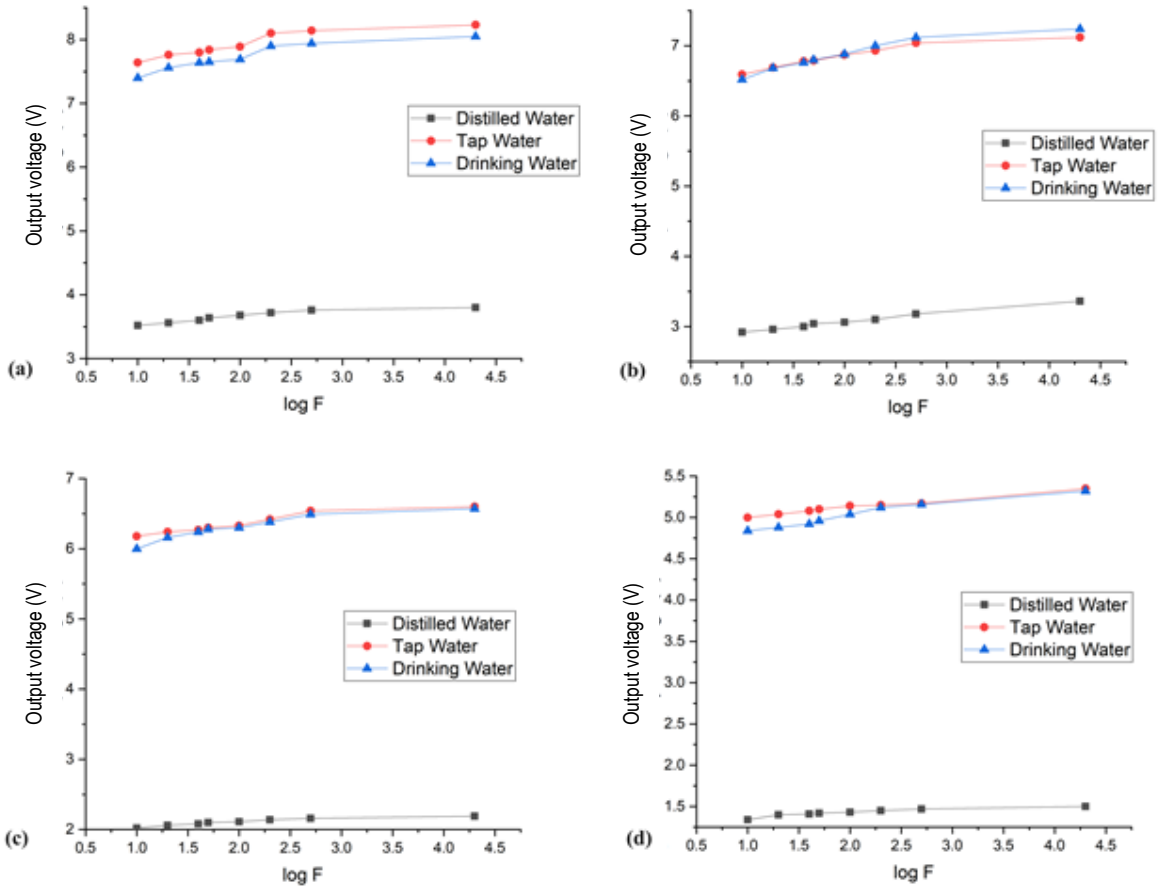

Figure 9. Frequency vs output voltage plot using different types of water as dielectric for (a) C_1, (b) C_3, (c) C_7, and (d) C_{15}

Table 2. The equations to determine the change in capacitance with respect to different concentrations of salinity levels at 20 kHz frequency

Sensor	Equation	R^2
C_1	y = -0.0093x + 9.8572	0.95
C_3	y = -0.0076x + 9.7676	0.97
C_7	y = -0.0097x + 9.7595	0.97
C_{15}	y = -0.0094x + 9.6768	0.92

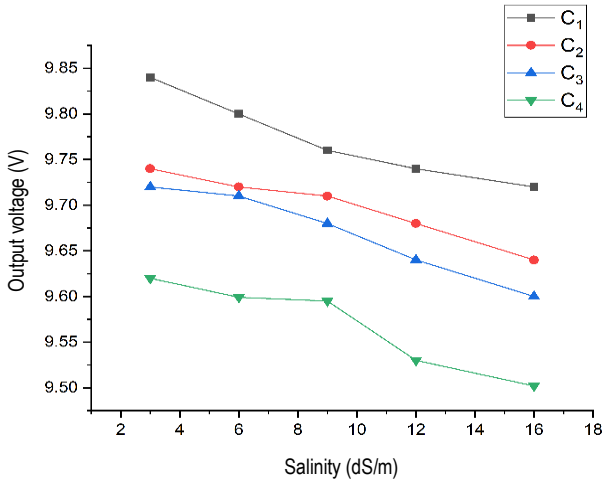

Figure 10. Salinity level vs output voltage plot at 20 kHz frequency

4. CONCLUSION

In this work, the authors successfully designed, simulated, and fabricated four different configurations of IDT capacitive sensors. An analog front-end, charge-to-voltage conversion circuit, for measuring the capacitance has been developed. The sensors responded with several millivolts when the frequency was varied using air and different types of water (including saline water) as the dielectric medium. It was found that the output voltage of the sensors changed with the change in water type and that the 1-1-1 configuration had the highest output voltage, whereas 1-15-1 had the lowest.

However, the sensors provided a negative linear response with different water salinity levels, i.e., when the salinity level was the highest, the observed output voltage was the lowest. In this study, IDT sensors were used only for contact-type water salinity level measurement. Further study needs to be performed as a future extension of this work to observe the non-contact type fringing field capacitance measurement.

ACKNOWLEDGMENT

Authors would like to thank the Department of Science & Technology (DST) and University Grant Commission (UGC), Government of India. The authors express sincere gratitude, in particular, to the invaluable support received from the Department of Instrumentation & USIC, Gauhati University.

REFERENCES

Akter, S. (2019). Impact of drinking water salinity on children's education: Empirical evidence from coastal Bangladesh. *Science of the Total Environment*, 690, 1331–1341.

Alam, A., Ullah, H., Attia, A., and Datta, A. (2020). Effects of salinity stress on growth, mineral nutrient accumulation and biochemical parameters of seedlings of three citrus root-stocks. *International Journal of Fruit Science*, 20(4), 786–804.

Baath, G. S., Shukla, M. K., Bosland, P. W., Steiner, R. L., and Walker, S. J. (2017). Irrigation water salinity influences at various growth stages of *Capsicum annuum*. *Agricultural Water Management*, 179, 246–253.

Bhat, S. (2005). *Salinity (conductivity) sensor based on parallel plate capacitors.* Doctoral dissertation. University of South Florida, United States.

Briggs, S. V., and Taws, N. (2003). Impacts of salinity on biodiversity—clear understanding or muddy confusion? *Australian Journal of Botany*, 51(6), 609–617.

Corwin, D. L. (2021). Climate change impacts on soil salinity in agricultural areas. *European Journal of Soil Science*, 72(2), 842–862.

Dasgupta, S., Huq, M., and Wheeler, D. (2016). Drinking water salinity and infant mortality in coastal Bangladesh. *Water Economics and Policy*, 2(1), 1650003.

Gadani, D. H., Rana, V. A., Bhatnagar, S. P., Prajapati, A. N., and Vyas, A. D. (2012). Effect of salinity on the dielectric properties of water. *Indian Journal of Pure & Applied Physics,* 50, 405–410.

Goswami, M. P., and Sarma, U. (2015). Analog frontend for fringe field capacitive soil moisture sensor. *Journal of Basic and Applied Engineering Research*, 2(19), 1698–1702.

Goswami, M. P., Montazer, B., and Sarma, U. (2018). Design and characterization of a fringing field capacitive soil moisture sensor. *IEEE Transactions on Instrumentation and Measurement*, 68(3), 913–922.

Islam, T., Maurya, O. P., and Khan, A. U. (2021). Design and fabrication of fringing field capacitive sensor for non-contact liquid level measurement. *IEEE Sensors Journal*, 21(21), 24812–24819.

Master, A. (2010). *Design and implementation of a signal conditioning operational amplifier for a reflective object sensor*. Master's thesis. University of Tennessee, United States.

Metternicht, G. I., and Zinck, J. (2003). Remote sensing of soil salinity: Potentials and constraints. *Remote sensing of Environment*, 85(1), 1–20.

Mizuguchi, J., Piai, J. C., de França J. A., de Morais França M. B., Yamashita, K., and Mathias, L. C. (2015). Fringing field capacitive sensor for measuring soil water content: Design, manufacture, and testing. *IEEE Transactions on Instrumentation and Measurement*, 64(1), 212–220.

Mohanavelu, A., Naganna, S. R., and Al-Ansari, N. (2021). Irrigation induced salinity and sodicity hazards on soil and groundwater: An overview of its causes, impacts and mitigation strategies. *Agriculture*, 11(10), 983.

Peddinti, S. R., Hopmans, J. W., Najm, M. A., and Kisekka, I. (2020). Assessing effects of salinity on the performance of a low-cost wireless soil water sensor. *Sensors*, 20(24), 7041.

Qian, Y., Zhao, Y., Wu, Q.-L., and Yang, Y. (2018). Review of salinity measurement technology based on optical fiber sensor. *Sensors and Actuators B: Chemical*, 260, 86–105.

Rahimi, L., Amanipoor, H., and Battaleb-Looie, S. (2021). Effect of salinity of irrigation water on soil properties (abadan plain, SW Iran). *Geocarto International*, 36(16), 1884–1903.

Rahman, M. H., Lund, T., and Bryceson, I. (2011). Salinity impacts on agro-biodiversity in three coastal, rural villages of Bangladesh. *Ocean & Coastal Management*, 54(6), 455–468.

Sharma, C., Dey, A., Khatun, H., Das, J., and Sarma, U. (2023). Design and development of a gas sensor array to detect salinity stress in Khasi Mandarin Orange plants. *IEEE Transactions on Instrumentation and Measurement*, 72, 2006409.

Wu, S., Lan, H., Liang, J.-J., Tian, Y., Deng, Y., Li, H.-Z., and Liu, N. (2015). Investigation of the performance of an inductive seawater conductivity sensor. *Sensors & Transducers Journal*, 186(3), 43–48.